Int. J. Electrochem. Sci., 12 **(2017)** 1535 – 1549, doi: 10.20964/2017.02.60

International Journal of
ELECTROCHEMICAL
SCIENCE
www.electrochemsci.org

Investigations on Corrosion Behaviour of WC–CrC–Ni Coatings Deposited by HVOF Thermal Spraying Process

Alin Constantin MURARIU[1,*], *Nicoleta PLEŞU*[2], *Ion Aurel PERIANU*[1], *Milica TARĂ-LUNGĂ-MIHALI*[2]

[1] National R&D Institute for Welding and Material Testing - ISIM Timisoara, 30 Mihai Viteazul Blv. 300222 Timisoara, Romania
[2] Romanian Academy, Institute of Chemistry, Timisoara, 24 Mihai Viteazul Blv. 300223 Timisoara, Romania
[*]E-mail: alin@isim.ro

Received: 22 November 2016 / *Accepted:* 24 December 2016 / *Published:* 30 December 2016

The paper presents investigations performed on WC–CrC–Ni coatings, deposited by High Velocity Oxygen Fuel (HVOF) thermal spraying, in order to assess the corrosion behaviour of coatings obtained using WOKA 7504 powder. Mechanical tests, structural and electrochemical analyses have been performed in order to determine the degree in which material composition, powder production method and technological parameters of HVOF process affect the corrosion resistance of the deposited layers. For the corrosion resistance, assessment electrochemical methods were used. Samples immersed in 3% NaCl solution and open-circuit potential (OCP) method were used to examine the potential change and creation of a protective layer on the surface. The best results, in terms of corrosion resistance and adherence resistance of the coating layer, were obtained for layer thickness of 110 to 220 μm. It was found that surface processing, after layer deposition through HVOF process, increases the corrosion rate about 1.5 times compared to unpolished ones, as a result of the protective passivated film removal that forms on the coating layer surface or due to the possibility of additional defects inducing in the deposited layer during the surface finishing operation.

Keywords: corrosion, electrochemical test, coatings, HVOF thermal spray, WC–CrC–Ni

1. INTRODUCTION

Corrosion, erosion and material fatigue are the main degradation mechanisms that lead to early failure and disposal of the components. Since these phenomena occur, due to undesired changes, starting from the material surface, these changes appear as an effect of chemical and electrochemical reactions (in case of corrosion), interaction of the material with the working environment (in case of

erosion) and cracks appearance (in case of fatigue). The necessity of proper protection of the base material by coatings is now a modern method and is extensively used in diverse applications: in the automotive industry, aviation industry, petrochemical and chemical industry, energy, construction, medical devices, internet and telecommunications as well as in the consumer goods industry.

Compared to the usual surfaces protecting methods such as metalizing, plating, enamelling, galvanizing or cathode protection [1-7], thermal spray coating is an innovative technology with low environmental impact, which allows covering any kinds of metallic or non-metallic surfaces using powders of advanced materials. Thus, to prevent the synergic effect of erosion - corrosion, currently special innovative composite materials for ceramic-metallic coatings, called "cermet" are used (WC–Co–Cr, WC–C–Ni or WC–Co). These coatings are successfully applied in the chemical and petrochemical industry where corrosive fluids are circulating containing particles (e.g. sand) that causes erosion [8].

The ceramic particles of cermet (carbides W or Cr) confer high erosion resistance of the mixture and higher plasticity properties of the metal matrix, compared with the case where coverage would be realized only with ceramic material. These composite materials could be deposited using Electric Arc (EArc), Atmospheric Plasma Spray (APS) or High Velocity Oxygen Fuel (HVOF) spraying method, technique in which the obtained layers are denser and more adherent [9, 10] due to the higher kinetic energy of the sprayed particles. Since in recent years new sorts of composite materials with special properties have been elaborated, this innovative technology for materials and products protection known an accelerated development, so far research in this area is focused on the study of corrosion - erosion mechanisms and characterization of the physicochemical [11] and mechanical stress behaviour [12-13] of the protective layers made from advanced coating materials, in order to improve the protective layer deposition technologies and to eliminate the negative effects and its related costs.

Improved corrosion resistance was reported for HVOF coatings if metallic and other binders were incorporated within the WC based matrix, Cr was added to the WC - Co or NiCrAl coatings and / or a post melt treatment was conducted [14-22].

The literature presents results concerning corrosion behaviour of HVOF coatings for tests conducted in either acidic or saline media [16, 17]. The corrosion processes were reported to be result of matrix composition, deficiency in homogeneity of binder matrix or coatings porosity. In acidic media the dissolution of the binder phase (Co) occurred during anodic polarization and activates the corrosion process, while the observed pseudo-passivity was associated with oxidation of the W, Co and C. The improved corrosion behaviour for WC-Ni composites coatings was ascribed to the Ni binder and lower porosity of these coatings.

The aim of this paper is to study the corrosion behaviour of WC–CrC–Ni coating layer, using electrochemical methods, mechanical tests and structural analysis, in order to assess the degree in which technological parameters of HVOF process and by default the coating thickness affect the corrosion resistance.

2. EXPERIMENTAL WORK

2.1 Material and methods

The tests were performed on samples taken from WC–CrC–Ni coating layers, deposited on S235JR carbon steel plates and on AISI 304 L stainless steel plates as substrate, with 4 mm thickness, using HVOF process. WOKA 7504 powder was used in order to achieve the coating layers. Materials used for this type of process are powdery and are appropriately designed to generate optimal quality of deposited layer. The main characteristics of the powder: chemical composition, size and distribution of the powder particle as well as powder production method have a significant impact on the technological characteristics of thermal spraying and hence on the quality of the deposited layers. For these reasons WOKA 7504 powder has been selected for testing since it contains spheroidal particles and is obtained by agglomeration and sintering. It has a uniform distribution of 43% chromium carbide and 37% tungsten carbide. The chemical composition and characteristics of the powders are presented in Table 1 and Table 2, respectively.

Table 1. Chemical composition / particle distribution and apparent density, manufacturer's data [%]

Powder	Cr	Ni	Co	C	Fe	W
WOKA 7504	38.5 – 43.5	10.0 – 13.0	2.9 – 4.1	7.7 – 8.5	< 0.5	the rest

Table 2. Characteristics of the powder WOKA 7504, manufacturer's data

Characteristics of the powder WOKA 7504	
Classification	Cr and W carbides
Chemical composition	Cr_3C_2 37WC 18Metal Alloy
Manufacturing method	Agglomeration and sintering
Morphology	Spheroidal
Dimensions	10 to 30 μm
The aspect	Rough
Apparent density	3.1 – 3.8 $g \cdot cm^{-3}$
Operating temperature	< 700 °C
Role	Corrosion and wear resistant
Recommended process	HVOF

2.2 Experimental setup

An experimental program has been developed for the obtaining of deposited layers with controlled thickness using an experimental setup consisting of specialized HVOF equipment which has a control module of the facility, a powder feeder and a spray gun, mounted on a robotic arm.

The cermet layer thickness depends on many parameters of the thermal spraying process. The studied cermet coatings were obtained by maintaining some parameters constant (in the recommended

range by the equipment manufacturer): gas flow: air (200 l·min^{-1}), oxygen (185 l·min^{-1}) and propane (68 l·min^{-1}), spraying gun – piece offset (225 mm), the powder flow (60 g·min^{-1}), the spraying gun travel speed (75 mm·s^{-1}) and the step between two successive run was calculated, on the basis of the deposited material distribution by spraying in the given conditions.

The notation of studied samples, number of deposited layers, powder flow and thickness of deposited layers are presented in Table 3.

To assess the correlation between structural aspects, mechanical characteristics and electrochemical properties, standard mechanical testing equipments and optical microscopes were used such as: EDZ 40 universal testing machine, ZWICK 3212 hardness apparatus, MAK-MS stereo microscope, MeF2 optical microscope. Electrochemical tests were performed using Autolab 302N EcoChemie after immersing the iron electrode for 1 h in 3% NaCl solution. The *Dcorr* cell corrosion cell contains the working electrode (exposed area of 0.785 cm^2) mounted in a Teflon holder, two stainless steel bars for counter electrodes and reference electrode Ag / AgCl in a Luggin capillary placed closely to the working electrode.

Table 3. Sample identification

No. crt.	Sample Identification	Observation
1.	MB	Base material, AISI 304 L stainless steel
2.	MB polished	Base material, AISI 304 L stainless steel, polished
3.	MB-OL	Base material, S235JR carbon steel
4.	MB-OL polish	Base material, S235JR carbon steel, polished
5.	S0	1 layer, 5 g·min^{-1}
6.	S1	1 layer, 60 g·min^{-1}, 114 μm
7.	S2	2 layers, 60 g.min^{-1}220 μm
8.	2 polish	2 layers, 60 g·min^{-1}, 220 μm polished surface
9.	S4	4 layers, 60 g.min^{-1}, 417 μm
10.	S4 polish	4 layers, 60 g·min^{-1}, 417μm polished surface
11.	S6	6 layers, 60 g·min^{-1}, 647 μm
12.	S6 polish	6 layers, 60 g·min^{-1}, 647 μm polished surface

The variation in time of open-circuit potential (*OCP*), from the first moment of sample immersion, was recorded in a free saline aerated solution. The polarization curves were obtained by scanning the potential of iron from -1200 to 200 mV at a scan rate of 1 mV/s. Corrosion parameters (corrosion potential – *Ecorr*, corrosion density current – *Jcorr*, polarization resistance – *Rp* and corrosion rate – *Rcorr*) were extracted from Tafel plots. The equivalent weight E_W was measured in grams/equivalent sample (E_W = 27.96 grams·equivalent^{-1}) and d represents the density in g·cm^{-3} (6.36 g·cm^{-3}).

EIS measurements were conducted under potentiostatic mode, around *OCP* values, at 22 ± 1 °C and impedance data was modelled by an equivalent electric circuit. Simulation program Zview – Associated Scribner Inc. and Levenberg - Marquard procedure was used for complex nonlinear simulation [23].

3. RESULTS AND DISCUSSION

The WOKA 7504 powder has been sprayed on base material by high velocity oxygen fuel (HVOF) technique to produce coatings with different thickness, ranging between 114 and 647 μm. Different numbers of cermet layers were successively deposited on the surface. Another set of sample after HVOF process deposition had the surfaces polished to a mirror finish. The correlation between thickness and number of layers is presented in Table 3. In the sample notation the value represents the number of deposited layers. The polished sample is marked with the notation polish.

The results of the adhesion tests of HVOF process, deposited coatings with WOKA 7504 powder, (both on carbon steel and stainless steel substrate), indicate a decrease of coating adherence with the increase of number of deposited layers (thickness of coating). The adherence resistance for S1 and S2 was 35.8 $N \cdot mm^{-2}$, very closed to adhesive resistance (37.5 $N \cdot mm^{-2}$) and 16 $N \cdot mm^{-2}$ for S6. These values indicate good adhesion resistance in the case of coating layers with a thickness of 100 to 220 μm (S1, S2) and poor adhesion resistance for coatings with the increased number of deposited layers.

Figure 1a presents the macroscopic aspects of the fracture surface appearance of coating S2 obtained by HVOF deposition for two successive layers of WOKA 7504 powdery material, after the adhesion test. The separation surface presents a mixed fracture aspect. Failure has occurred both in adhesive (dark grey) and at the interface between deposited material and substrate (light grey).

a) Deposited layers of sample S2 b) Deposited layers of sample S6

Figure 1. Fracture surface appearance of the samples after the adhesion test

In the case of sample S6, with 6 deposited successive layers (Figure 1b), the separation surface presents a mixed failure, carried out mainly at the interface between deposition and substrate, but also between successively deposited layers. A deep coloration of substrate was observed, meaning that during the deposition process the sample was excessively heated. Cracks were highlighted at the macroscopic level in the coating.

At macroscopic level, in the sample coatings with low number of successive layers (one or two layers) no imperfections were observed at the interface between the deposited material and substrate. Only fine pores were observed in the deposited material and, at microscopic level, some fine cracks.

Coatings containing low number of layers seem to present practically the same structure and microstructure and their mechanical properties can be expected to be similar. By increasing the number of layers in coatings (4 or 6 successive layers: S4 and S6 samples), in addition to the existing pores between the layers, observed for S0, S1 and S2 samples, defects as lamellar boundaries, intra and inter-layer cracks appear. Figure 2a presents the micro structural aspect for sample S2 and shown very good penetration of the coating into the substrate. Figure 2b presents the micro structural aspect of deposited layer, for sample S6 and indicates some cracks developed perpendicular to the layers and propagated toward the outer surface of the deposition. These aspects, in conjunction with the average adhesive strength of only 16.0 $N.mm^{-2}$, emphasizes that in this case the adherence of deposited layer to substrate is very low.

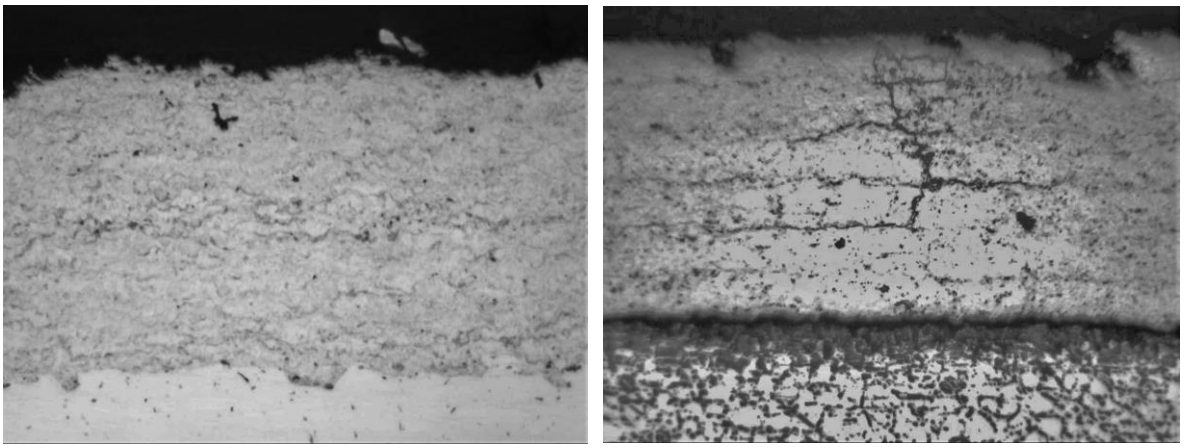

a) Sample S2 [100×] **b)** Sample S6 [50×]

Figure 2. Microstructural appearance of deposited layers

Hardness tests conducted under the experimental program have shown that by depositing of protecting coatings, the surface coatings hardness increases by 5 to 9 times. These obtained coatings showing higher hardness values (766 to 1355 HV1) comparatively with the substrate (148 to 216 HV1). The best results in terms of hardness were obtained for the coatings containing two layers, having an average thickness of 220 μm.

Qualitatively information regarding capability of corrosion protection offered by coatings was obtained from the variation in time of *OCP* potential (Figures 3a and b).

It was observed for all samples that the *OCP* value decreased in time as a result of dissolution of passive oxide layer formed at the sample surface (electrodes), explained by the destructive chloride ions attack. In time, a partially protection of surface took place by formed corrosion species capable to block the existing pores and cracks from the sample surface and conducted to potential stabilization. In the case of MB surface, the *OCP* values increased with the immersion time and, after 250 s, reached a constant potential value.

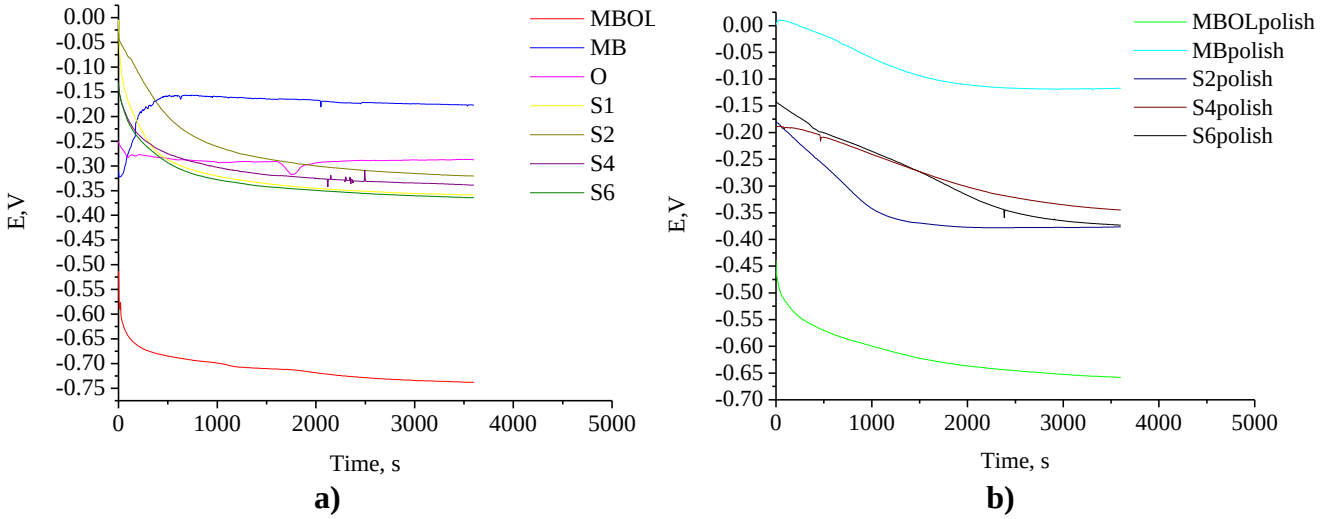

Figure 3. The variation of *OCP* potential with immersion time for electrodes with a) unpolished surface and b) polished surface in 3% NaCl solution at 22 ± 1 °C.

In the case of unpolished surfaces, the *OCP* potential tended to stabilize more slowly (approx. 750 s), (Figure 3a). For polished electrodes, MB and MB-OL the *OCP* value was stabilized after 2000 to 2500 s immersion in saline solution (Figure 3b). The higher time needed for *OCP* stabilization in the case of polished surface comparatively with unpolished ones was a result of increased number of cracks, defects and lamellar boundaries, as consequence of the mechanical stress induced by polishing.

The potentiodynamic polarization curves obtained for substrate and coatings obtained by HVOF process and subsequent polishing, after 90 min immersion in saline solutions, are shown in Figures 4a and b.

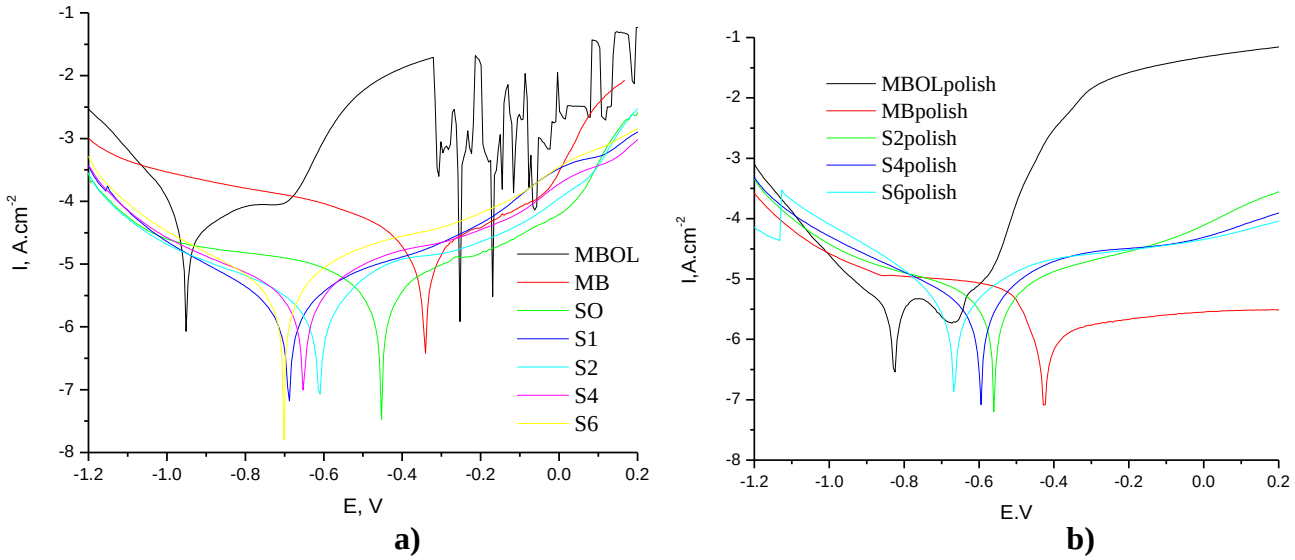

Figure 4. Polarization curves samples a) unpolished surface and b) polished surface after 90 min immersion in 3.0 wt % NaCl solutions at 22 ± 1 °C.

From the data, it is clear that the corrosion potential (*Ecorr*) of MB-OL sample (-0.923 V vs. Ag/AgCl) is shifted towards positive region, while the surface of steel has been coated with the cermet,

and the shift was less accentuated with the increase of layers in thickness. For coatings with one layer (S1) the *Ecorr* is -0.679 V and for coatings with six layers (S6) the *Ecorr* was -0.709 V, while comparing the *Ecorr* values of these two coatings, S1 showed more positive *Ecorr* values than those of S6. This is in accordance with other studies on coatings where negative values for the free corrosion potential were reported. This feature assigns for these HVOF coatings an opportunity to be used as sacrificial coatings in saline surroundings [24, 25].

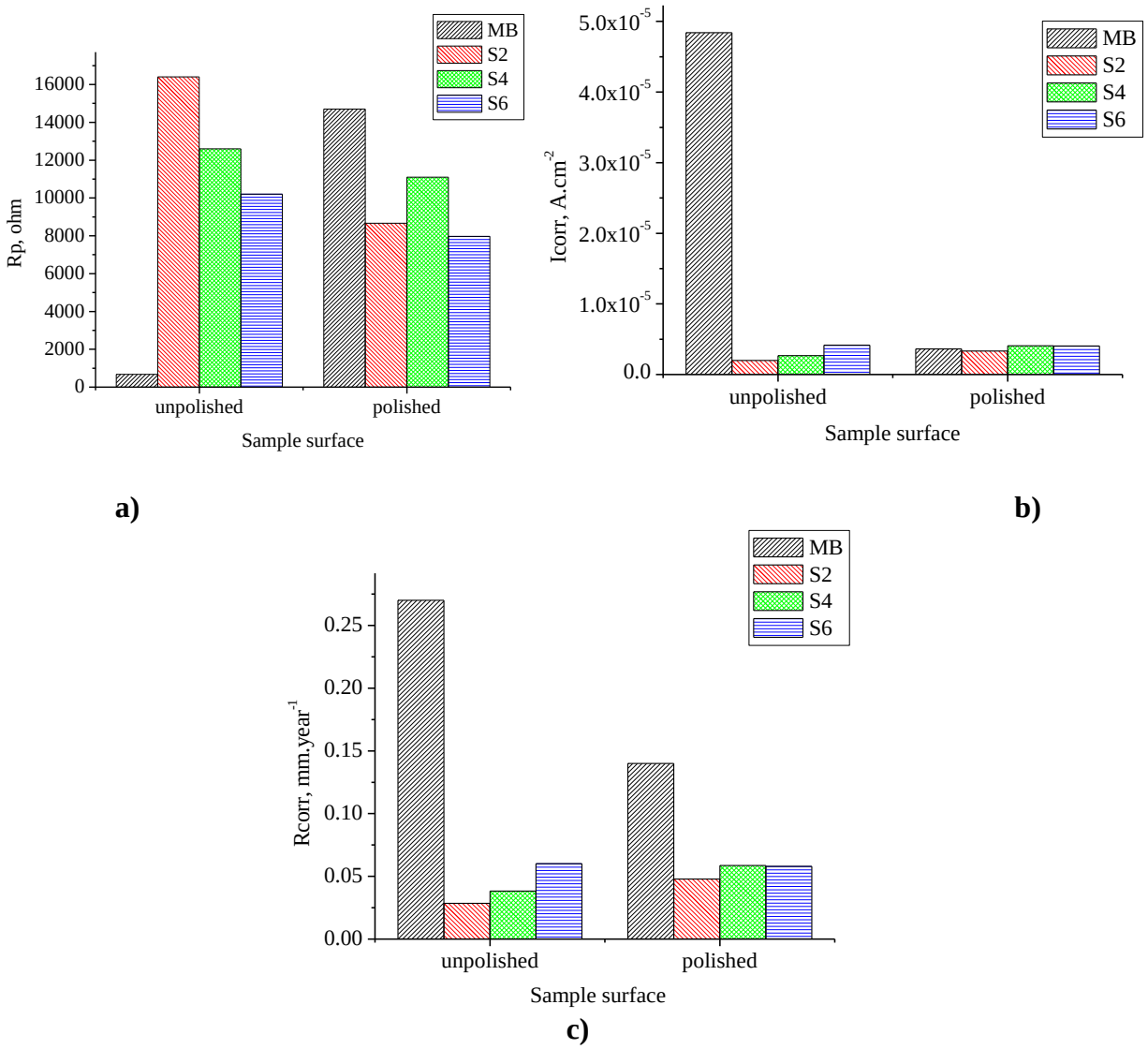

Figure 5. Variation of: a) polarization resistance (*Rp*), b) Corrosion density currents (*Icorr*) and c) Corrosion rates (*Rcorr*) and comparatively for unpolished and polished samples in 3% NaCl solution at 22 ± 1 °C.

Experimental data indicates an increase of polarization resistance and decrease of corrosion rate and corrosion current for all coated samples relatively with uncoated ones.

Polarization resistance, corrosion rate and corrosion current depend on the number of coating layers and if the surface of sample is further polished or not after the HVOF process. The lower corrosion rates and corrosion currents density are observed in the case coatings with one or two layers

and on unpolished surface samples. The corrosion current density is a key parameter that suggests the capacity of coating in protecting substrates against electrolyte aggressiveness, and is inversely proportional to the polarization resistance.

The corrosion currents density *Icorr* are low for all coated samples comparatively with uncoated ones (Figure 5b). The values for S1, S2 and S2–polish samples are $1.26 \cdot 10^{-6}$ A·cm^{-2}, $1.975 \cdot 10^{-6}$ A·cm^{-2} and $3.32 \cdot 10^{-6}$ A·cm^{-2}, respectively. Similar value was reported for a multilayer film WC–12Co coated sample obtained from commercial WOKA 3102 powder, which shows an *Icorr* value about $7 \cdot 10^{-6}$ A·cm^{-2} [26] and for other W–Cr–C composite [27].

The results from this study indicate lower *Icorr* values for deposits with 2 layers up to 6 times lower than other HVOF coatings (WC-12Ni, WC-20Cr2C3-7Ni and WC-10Co-4Cr respectively) with the same thickness [22]. Coatings prepared by Han and co-workers exhibit for WC−27NiCr and WC−10Co4Cr better corrosion resistance and the corrosion current densities of $4.3760 \cdot 10^{-8}$ A·cm^{2} and $4.7634 \cdot 10^{-7}$ A·cm^{2}, respectively [28].

An increase of *Icorr* was observed for polished surface, as a result the interfacial cracks development, and inter-connection of existing pores as a result of the supplementary mechanical stress. It was observed that the *Rp* increased, *Rcorr* and *Icor* decreased with the number of layers in the coating.

The electrochemical corrosion test results have shown that by depositing of a coating obtained with HVOF process, using WOKA 7504 powder, the corrosion rate of the surface material is significantly reduced (for unpolished surfaces after deposition) from $2.742 \cdot 10^{-1}$ mm·year^{-1} (MB) and of $5.615 \cdot 10^{-1}$ mm·year^{-1} (MB-OL) to only $1.815 \cdot 10^{-2}$ mm·year^{-1} for a deposited layer with a thickness of about 110 μm (S1) and of $2.846 \cdot 10^{-2}$ mm·year^{-1} for a layer thickness of 220 μm (S2), respectively.

It is expected that the coatings corrosion resistance to rise by increasing the coating thickness. It was reported for HVOF amorphous metallic coatings deposited on Fe substrate that if the coatings thickness rises from 100 to 450 μm, the passive current density decrease as an effect of through-pores formation, which are easier to create in a thinner coating [29].

Once the thickness of the deposited layer increases, the corrosion rate increases as well, reaching $6.011 \cdot 10^{-2}$ mm·year^{-1}, for layers with a thickness of 650 μm (S6). This is explained by the imperfections and cracks development in the thicker layers, as was highlighted by the structural analyses.

On the other hand, it was found that when the deposited layer was polished after the HVOF process, the corrosion rate increased significantly, thus, in the case of deposits with 2 layers the corrosion rate increased from $2.846 \cdot 10^{-2}$ mm·year^{-1} (S2) to $4.783 \cdot 10^{-2}$ mm·year^{-1} (S2-polish) and for 4 layers from $3.832 \cdot 10^{-2}$ mm·year^{-1} (S4) to $5.858 \cdot 10^{-2}$ mm·year^{-1} (S4–polish), respectively. These results indicate the increase of tension and number of cracks with the increase number of successive deposition layer in coatings and a sensitivity of properties with the spraying parameter.

The corrosion data is well correlated with the results obtained in fracture surface appearance of the samples, after adhesion tests and microstructure images.

Also, these defects in the coatings can be accentuated by a supplementary mechanical stress (polishing). Surface processing, after HVOF process layer deposition, enlarges the defects in coatings since the coating layer presents high hardness and therefore is fragile. In result, an increase of the

corrosion rate of about 1.5 times was observed. Similar observation was reported for cermet subjected to laser post heat-treatment which induces cracks and porosity [30].

The microstructure differences influence the *EIS* spectra. In Figures 6 the impedance spectra Nyquist graph (Figure 6a) shows the imaginary component of the impedance plotted as a function of the real component, and the Bode representation (Figure 6b) shows the logarithm of the impedance modulus $|Z|$ and phase angle as a function of the f frequency logarithm.

It can be seen for each *EIS* spectrum of samples the presence of two time constants since two peaks are observed in the Bode plots. This characteristic most likely appears from the volume shrinkage of ceramic and the generation of through-thickness cracks after the HVOF process. The solution could directly infiltrate to the substrate through these cracks and initiate the corrosion process. The complex plane (Nyquist) plots (Figure 6a) show a higher capacitive semicircle for sample S0 and S2, which indicates that the sample with low thickness presents the highest total impedance and the highest corrosion resistance, in agreement with the polarization measurement results. Figure 6b shows the Bode phase plots and illustrates two time constants, while bare surface samples present a well-defined time constant: one attributed to the coatings and the second to the corrosion process. Sample S2 shows this time constant at a lower frequency value (around 10^{-3} Hz) and a higher phase angle and points out to a better barrier performance.

The most commonly equivalent circuit used in many papers present for modelling of *EIS* data electrical equivalent circuits with two time-constant [31, 32]. The electric equivalent circuit (*EEC*) used to extract the electrochemical parameters is shown in Figures 7a and b. The first *EEC* models the behaviour of coatings and the second *EEC* models the bare substrate. The model presented in Figure 7a contains the resistance of electrolyte *Rs*, the resistance *R1* associated with ionic transfer in the coating pores and resistance *R2* the polarization resistance. *CPE1* models the charge/discharge process at the coating/electrolyte interface and *CPE2* represents the charge/discharge process that occurs at the substrate/electrolyte interface as a result of the electrolyte infiltration through the pores and creation of ionic conduction path across coating.

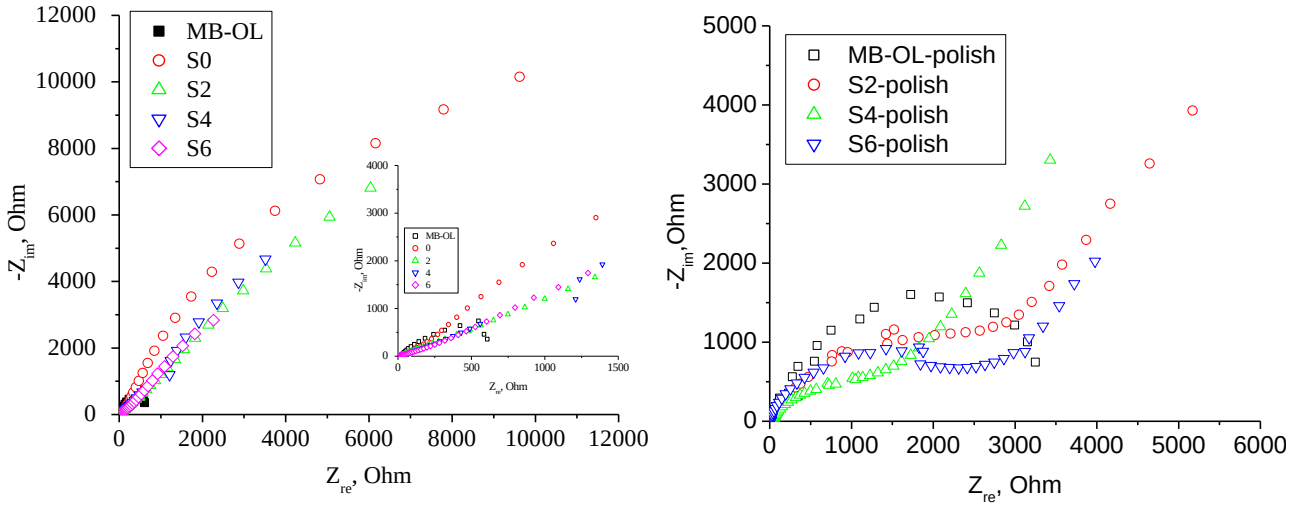

a)

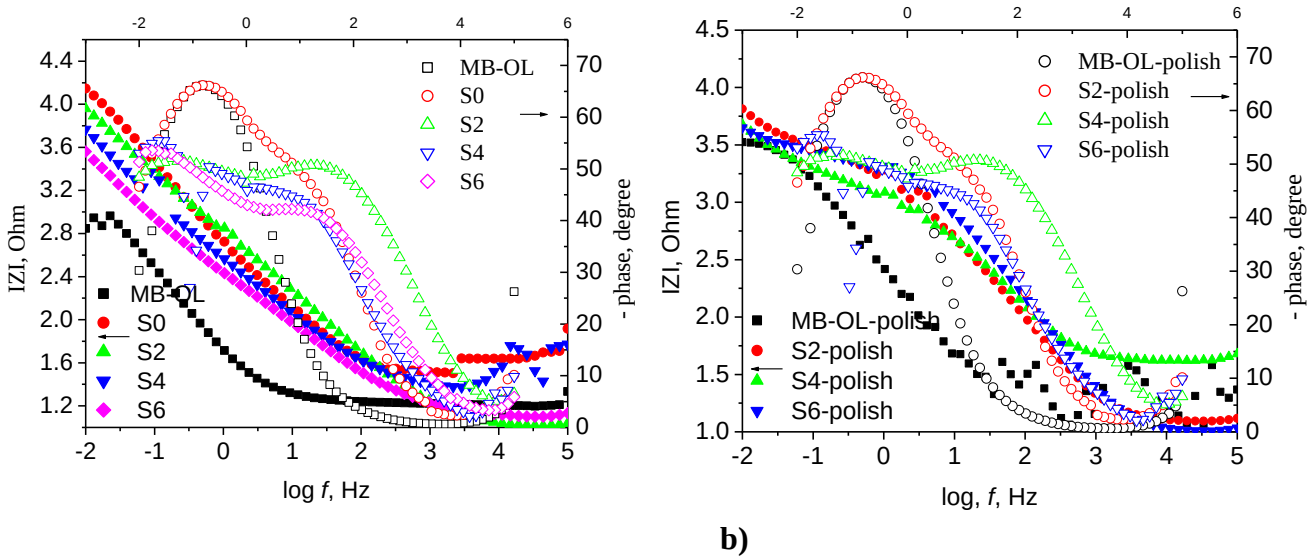

Figure 6. Impedance spectra: a) Nyquist graph and b) Bode representation (logarithm of the impedance modulus |*Z*| (fill symbols) and phase angle (hollow symbols) as a function of the logarithm of the frequency *f*, recorded in 3% NaCl solution at 22 ± 1 °C.

Constant phase element (*CPE*) was taken into consideration to represent the double layer capacitance, as a result of its non-ideal behaviour. The impedance of a *CPE* can be expressed by $Z_{CPE} = [T(j\omega)^n]^{-1}$, where ω is frequency; *T* is the *CPE* magnitude and the exponent *n* is between 0 and 1.

For substrate the data were modelled by a simple Randler circuit (Figure 7b) and contains only the resistance of electrolyte *Rs*, the resistance *R2* the polarization resistance and *CPE*2 represents the charge/discharge process that occurs at the substrate/electrolyte interface.

The value of *R1* is a measure of pore size in coatings; higher values indicate a lower size and *R2* value is linked to the micro structural patterns and describes the ability of the coating to restrain ion transfer at the solution/coating interface.

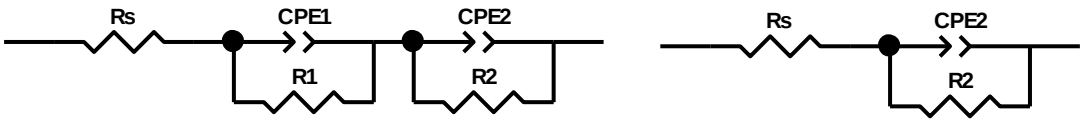

Figure 7. Schematic representation of the electric equivalent circuit for: a) coatings and b) for substrate

The values of *EIS* parameters for samples are presented in Table 4.

The impedance data for coated sample correspond well to the model, shown in Figure 7a, and the substrate in Figure 7b. The value for *R1* corresponds to the resistance of coatings and increase with the coating thickness and decrease with the increase of pore number and size. The high value of *R1* was obtained in the case of S2 sample and indicates a good coating with small pore size, comparatively with S6 sample which is more porous.

Table 4. The value of *EIS* parameters

Samples	Chi-Sqr	Sum-Sqr	*Rs*, Ω·cm^2	*CPE1-T*, F/cm^2/sϕ^{-1}	*CPE1-P*(+),(ϕ)	*R1*(+), Ω·cm^2	*CPE2-T* F/cm^2/sϕ^{-1}	*CPE2-P*(+),(ϕ)	*R2*(+), Ω·cm^2
S2	$7.91 \cdot 10^{-04}$	0.02	9.72	$7.39 \cdot 10^{-04}$	0.62	468	$6.55 \cdot 10^{-04}$	0.68	42620
S2-polish	$8.77 \cdot 10^{-03}$	0.27	11.71	$7.18 \cdot 10^{-05}$	0.79	226	$1.19 \cdot 10^{-03}$	0.70	12523
S4	$2.41 \cdot 10^{-01}$	6.99	35.16	$5.58 \cdot 10^{-04}$	0.83	153	$1.15 \cdot 10^{-03}$	0.73	11798
S4-polish	$8.12 \cdot 10^{-03}$	0.25	40.07	$8.30 \cdot 10^{-05}$	0.76	141	$1.27 \cdot 10^{-03}$	0.63	10120
S6	$3.73 \cdot 10^{-04}$	0.01	12.35	$1.47 \cdot 10^{-03}$	0.56	215	$1.81 \cdot 10^{-03}$	0.69	9237
S6-polish	$5.17 \cdot 10^{-03}$	0.16	9.633	$3.50 \cdot 10^{-05}$	0.83	215	$1.56 \cdot 10^{-03}$	0.71	3769
MB-OL	$1.27 \cdot 10^{-02}$	0.43	16.65	-	-	-	$4.73 \cdot 10^{-03}$	0.82	2742
MB-OL-polish	$2.90 \cdot 10^{-01}$	9.27	18.9	-	-	-	$8.45 \cdot 10^{-04}$	0.83	3941
MB	$8.06 \cdot 10^{-03}$	0.27	12.06	-	-	-	$5.45 \cdot 10^{-04}$	0.80	1658
MB-polish	$3.79 \cdot 10^{-01}$	12.8	10.69	-	-	-	$2.31 \cdot 10^{-05}$	0.94	2650

The polarization resistance *R2* is linked by *R1* which is a measure of quality of coating because a lower value of *R1* reflects a greater possibility of a reaction at the interface.

R2 decreases with the increase of number and size pores within the coating film. Higher values of *R2* indicate a coating/electrolyte interface with lower open porosity and, accordingly, less susceptible to corrosion. This result validates an improved corrosion resistance of HVOF deposited layer compared to uncoated surface. The layer with 110 to 220 μm thickness showed an enhanced corrosion protection performance compared to the coatings with higher thickness. The mechanical stress after layer deposition allowed the interconnection of the existing pores and makes the surface more prone to chlorine aggressive attack. The observation regarding the existing of a critical thickness of the cermet interlayer and the interrelation with its corrosion protectiveness was reported in literature. Barleta and Bolelli [33, 34] reported analogous behaviour for coatings where WC–CoCr layers are thinner (around 100 μm) and present too much interconnected porosity which is not able to prevent the beginning of corrosion of the substrate. Our experimental data, also, support these observations regarding the existence of a critical thickness of the cermet interlayer and, also, the existence of a correlation between thickness of cermet layers and its corrosion protectiveness.

The results of potentiodynamic polarization further support the results of electrochemical impedance spectroscopy and also indicate that coatings with 110 to 220 μm thickness are the more resisting to aggressive chlorine attack.

The surface properties of WC-CrC-Ni coatings obtained by optimal coating process were previous investigated by W. Fang and co-workers [35] and by M. M. El Rayes and co-workers [9]. They found that the HVOF sprayed WC–CrC–Ni coating is very protective for the substrate, has a good thermal stability and corrosion resistance due to its better compaction and low chemical decomposition of powders. M. M. El Rayes and co-workers concluded that chemical composition of metallic binder materials and the occurrence of micro cracks were the most important factors influencing the corrosion resistance of the HVOF sprayed WC coatings in the strong acidic environment.

Results obtained in the current paper have allowed validating the hypothesis that in saline environment, as in case of a strong acidic environment, the occurrence of pores and micro-cracks in HVOF sprayed WC-CrC-Ni coatings, represents the main factor influencing corrosion resistance and

the existence of a critical thickness and a correlation between thickness of cermet layers and its corrosion protectiveness. Additionally, it was also revealed that occurrence of micro-cracks and, therefore, corrosion resistance is closely related to HVOF thermal spraying process parameters that change deposited layer thickness.

4. CONCLUSIONS

The paper illustrates the relevance of combining results of mechanical testing, micro structural analysis with chemical and electrochemical evaluation, in order to obtain relevant information on corrosion behaviour of WC–CrC–Ni coatings deposited by HVOF process. The layers deposited by HVOF using this type of powder are dense, have a good adhesion resistance, are homogeneous which gives them a high hardness and a good corrosion resistance and thus can be used to protect pumps, pipes and other components used the chemical industry, as an alternative to hard chrome plating.

In case of WC–CrC–Ni coatings deposited by HVOF process, using WOKA 7504 powder, the existence of a critical thickness and a correlation between thickness of cermet layers and its corrosion protectiveness was observed; the best experimental results on adhesion and corrosion resistance were obtained for layer thickness of 110 to 220 μm. For lower coating layer thickness, the corrosion resistance decreases continuously, due to the fact that the corrosive agent can easily infiltrate through the substrate, since the deposited layer is porous. Once the coating layer thickness increase to over 400 to 650 μm, coating imperfections occur and leads to the reduction of the corrosion resistance and even cause layer cracking.

A decrease of corrosion rate and corrosion current, for all coated samples, were observed.

Polarization resistance, corrosion rate and corrosion current depend on the number of coating layers and if the surface of sample is further polished or not. In general, it was observed that the *Rp* increase, *Rcorr* and *Icor* decreases with the number of layers in the coating.

Surface processing after layer deposition through HVOF process, increase the corrosion rate about of 1.5 times, as an effect of the protective passivated film removal that forms on the coating layer surface or due to the likelihood of additional defects inducing in the deposited layer during the surface finishing operation, since the coating layer has a very high hardness and therefore is fragile.

Lower corrosion rates and corrosion currents density are observed in the case of coatings with low number of layers (one or two layers) and on unpolished surface samples.

ACKNOWLEDGEMENTS

This study was supported by the Romanian National Authority for Scientific Research and Innovation, as a part of the project NUCLU PN 16 08 201. The authors would like to acknowledge support provided by the National R&D Institute for Welding and Material Testing - ISIM Timisoara and by the Romanian Academy, Institute of Chemistry, for all facilities necessary to implement the experimental research.

References

1. Y. Qian, Y. Li, S. Jungwirth, N. Seely, Y. Fang and X. Shi, *Int. J. Electrochem. Sci.,* 10 (2015) 10756.
2. D. Hernandez-Martinez, U. Leon-Silva and M.E. Nicho, *Anti-Corros. Methods Mater.,* 62 (2015) 229.
3. C. Deya, *J. Mater. Eng. Perform.,* 24 (2015) 1206.
4. H. R. Zhu, W. Tang, C. Z. Gao, Y. Han, T. Li, X. Cao and Z. L. Wang, *Nano Energy*, 14 (2015) 193.
5. W. X. Guo, X. Y. Li, M. X. Chen, L. Xu, L. Dong, X. Cao, W. Tang, J. Zhu, C. J. Lin, C. F. Pan and Z. L. Wang, *Adv. Funct. Mater.,* 24 (2014) 6691.
6. E. S. Sarac, G. Girgin, S. S. Palabiyik, M. Charehsaz, A. Aydin, G. Sahin and T. Baydar, *Biol. Trace Elem. Res.,* 151 (2013) 330.
7. F. Wang, J. Liu, Y. Li, R. Fan and Y. Li, *Int. J. Electrochem. Sci.*, 7 (2012) 3672.
8. M. M. El Rayes, H. S. Abdo and K. A. Khalil, *Int. J. Electrochem. Sci.*, 8 (2013) 1117.
9. L. Pawlowski, *The Science and Engineering of Thermal Spray Coatings, 2nd edition,* John Wiley & Sons Ltd., (2008) Chichester, U.K.
10. M. Rendón-Belmonte, J. T. Pérez-Quiroz, J. Terán-Guillén, J. Porcayo-Calderón, A. Torres-Acosta and G. Orozco-Gamboa, *Int. J. Electrochem. Sci.,* 7 (2012) 1079.
11. S. R. Taylor, G. A. Shiflet, J. R. Scully, R. G. Buchheit, W. J. VanOoij, K. Sieradzki, R. E. Diaz, C. J. Brinker and A. L. Moran, *ACS Symp. Ser.,* 1008 Ch. 8 (2009) 126.
12. Z. Lu, S. W. Myoung, Y. G. Jung, G. Balakrishnan, J. Lee and U. Paik, *Materials,* 6 (2013) 3387.
13. G. Umesh, B. Mallikarjun and C. S. Ramesh, *Int. J. Mech. & Ind. Tech.,* 2 (2015) 41.
14. P. M. Natishan, S. H. Lawrence, R. L. Foster and B. D. Sartwell, *Corrosion*, 58 (2002) 119.
15. B. D. Sartwell, *Adv. Mater. Process*, 156 (1999) 25.
16. A. Lekatou, E. Regoutas and A. E. Karantzalis, *Corros. Sci.*, 50 (2008) 3389.
17. A. Lekatou, D. Grois and D. Grimanelis, *Thin Solid Films*, 516 (2008) 5700.
18. P. K. Aw, A. L. K. Tan, T. P. Tan and J. Qiu, *Thin Solid Films*, 516 (2008) 5710.
19. J. M. Perry, T. Hodgkiess and A. Neville, *J. Therm. Spray Techn.*, 11 (2002) 536.
20. R. Saenger, D. Martin and C. Gabrielli, *Surf. Coat. Tech.*, 194 (2005) 335.
21. C. Godoy, M. M. Lima, M. M. R. Castro and J. C. Avelar–Batista, *Surf. Coat. Tech.*, 188-189 (2004) 1.
22. L. P. Ward, B. Hinton, D. Gerrard and K. Short, *JMMCE*, 10 (2011) 989.
23. http://www.scribner.com/ Electrochemical Impedance Spectroscopy measurements.
24. M. Metikos-Hukovic and R. Babic, *Corros. Sci.*, 49 (2007) 3570.
25. C. D. Arrieta-González, J. Porcayo-Calderon, V. M. Salinas-Bravo, J. G. Chacon-Nava, A. Martinez-Villafañe and J. G. Gonzalez-Rodriguez, *Int. J. Electrochem. Sci.,* 6 (2011) 3644.
26. C. Monticelli, A. Balbo and F. Zucchi, *Surf. Coat. Tech.,* 204 (2010) 1452.
27. Y. Jiang, J. F. Yang, Z. M. Xie, R. Gao and Q. F. Fang, *Surf. Coat. Tech.,* 254 (2014) 202.
28. M. Han, S. Lee, M. Kim, S. Jang and S. Kim, *T. Nonferr. Metal Soc.,* 22 (2012) s753.
29. A. Gisario, M.Barletta and F.Veniali, *Opt. Laser Technol.,* 44 (2012) 1942.
30. H. S. Ni, X. H. Liu, X. C. Chang, W. L. Hou, W. Liu and J. Q. Wang, *J. Alloy. Compd*., 467 (2009) 163.
31. Y. Sun, J. E. Remias, X. Peng, Z. Dong, J. K. Neathery and K. Liu, *Corros. Sci.*, 53 (2011) 3666.
32. M. Azzi, M. Paquette, J. A. Szpunar, J. E. Klemberg-Sapieh and L. Martinu, *Wear* 267 (2009) 860.
33. M. Barletta, G. Bolelli, B. Bonferroni, L. Lusvarghi, *J. Therm. Spray Technol*., 19 (2010) 358.
34. G. Bolelli, B. Bonferroni, G. Coletta, L. Lusvarghi and F. Pitacco, *Surf. Coat. Tech.*, 205 (2011) 4211.

35. W. Fang, T.Y. Cho, J.H. Yoon, K.O. Song, S.K. Hur, S.J. Youn, H.G. Chun, *J. Mater. Process. Tech.*, 7 (2009) 3561.